Article ID: 1003－6326(2003)06－1360－07

Approximants in annealed IQC(Icosahedral Quasicrystal)-DQC(Decagonal Quasicrystal) pseudo-binary alloys①

LEI Yi(雷 奕)[1, 2], J. M. Dubois[2], M. Calvo-Dahlborg[2],
HEI Zu-kun(黑祖昆)[3], P. Weisbecker[2], DONG Chuang(董 闯)[1]
(1. State Key Laboratory for Materials Modification, Department of Materials Engineering, Dalian University of Technology, Dalian 116024, China;
2. LSG2M, CNRS-UMR7584, Ecole des Mines, Parc de Saurupt, 54042 Nancy Cedex, France;
3. Institute of Material & Technology, Dalian Maritime University, Dalian 116024, China)

Abstract: The structure and microstructure of constituent phases in annealed $IQC_{100-x}DQC_x$ alloys, made from mixtures of $Al_{62}Cu_{25.5}Fe_{12.5}$ icosahedral quasicrystal (IQC) and $Al_{70}Co_{15}Ni_{15}$ decagonal quasicrystal (DQC), were studied by X-ray diffractometry(XRD), scanning electron microscopy (SEM), and energy-dispersive X-ray spectroscopy (EDAX). These constituent phases are mostly approximants: λ, β and τ3. In addition, an Al-Cu-Co DQC phase is observed in $IQC_{80}DQC_{20}$ alloy. The nature of these approximants and their relationship with the quasicrystals(QCs) are discussed; and the evolution of these phases is interpreted by the shifting of their *e*/*a*-constant lines in the Al-(Cu, Ni)-(Fe, Co) pseudo-ternary phase diagrams.

Key words: quasicrystals; approximants; phase diagram; *e*/*a*-constant line
CLC number: TG 111.15; TG 113.12 **Document code:** A

1 INTRODUCTION

With nowadays improvement in the understanding of the quasicrystalline material, its potential applications have been gradually pointed out in various fields as thermal insulation[1], light absorption[2, 3], power generation[4] and hydrogen storage[5, 6], etc. Private companies have shown great interest especially in the application of its tribology and thermo-power generation properties. Therefore, better understanding of the scientific natures of quasicrystals (QCs) and its approximant is believed to become a good path that will finally leads to further discovery of many potential applications of this material.

The study of approximants is an effective way to investigate the structures and properties of related QCs. In addition to complex approximants like α-AlMnSi[7] and λ-$Al_{13}Fe_4$, some QC-related crystalline phases having simple structure (like B2[8] and τ3[9]) were also considered as approximants due to their similar valence concentration values to the corresponding QCs[10].

Structures of two major types of QCs, namely icosahedral quasicrystals (IQCs) and decagonal quasicrystals(DQCs), have already been studied quite extensively. In IQC, its basic cluster-icosahedra are arranged in quasiperiodic ways in three directions. While in DQC, the icosahedra are arranged in two dimensional quasiperiodic lattices. Although they belong to different types, they both contain icosahedral clusters as their common basic units.

Due to their structural similarities, the transformation from IQC to DQC occurs in many QC systems. This transition was first observed by Schaefer et al in the Al-Mn system[11]. Later, in the Al-Pd-Mn system, a high-temperature stable DQC phase was found to precipitate from a supersaturated IQC phase through a solid-state reaction[12].

In this paper, the mutual transition of these two different types of QCs is studied with different method: two representatives of these two types of QCs namely are mixed together and then melt in an induction furnace. Therefore, by studying the evolution of their phase constitutions in the mixed alloys, the way of interaction of their basic clusters can be investigated and the degree of disorders that has been introduced into original perfect quasiperiodic lattice structure can be estimated. These studies are considered to be beneficial to the future production of QC-based amorphous materials.

2 EXPERIMENTAL

Two stable quasicrystals, IQC-$Al_{62}Cu_{25.5}Fe_{12.5}$

① **Foundation item:** Project (PRA MX 99/04) supported by French-Chinese Association for Scientific and Technologic Research (AFCRST), French-Chinese Advanced Research Program on Materials; project(50071013) supported by the National Natural Science Foundation of China
Received date: 2002－12－16; **Accepted date:** 2003－03－24
Correspondence: LEI Yi, PhD; Tel: +86-411-4729791; Fax: +86-411-4708389; E-mail: lei_yi@yahoo.com

and DQC-$Al_{70}Co_{15}Ni_{15}$, were chosen as the two starting components for alloying. The two starting quasicrystalline ingots were prepared by melting respectively Al, Cu, Fe and Al, Co, Ni elements, with purities superior to 99.99%, in a high-frequency induction furnace under Ar atmosphere. The as-cast $Al_{62}Cu_{25.5}Fe_{12.5}$ ingot is further annealed at 750 ℃ for 2 h to remove the β phase impurity[13].

In experiment, eight $IQC_{100-x}DQC_x$ alloys were designed with x = 10, 20, 30, 50, 60, 70, 80 and 90 (mass fraction). Each alloy was obtained by melting x% of DQC-$Al_{70}Co_{15}Ni_{15}$ with (100− x)% of IQC-$Al_{62}Cu_{25.5}Fe_{12.5}$ in the same high-frequency induction furnace. For easy comparison, the correspondence between the compositions of the pseudo-binary alloys in mole fraction and in mass fraction are presented in Table 1. All the samples were cooled down slowly in the furnace by decreasing the current gradually after that the melt was sufficiently homogenized. The cooling rate is estimated to be about 1 K/s. The as-cast samples were subsequently annealed at 1 023 K for 1 h in a vacuum furnace to remove metastable phases.

The XRD analysis was carried out in an X-ray diffractometer (Siemens d500) with Co K_α source (λ= 0.178 896 5 nm) to identify existing phases in each alloy. The morphology and composition were determined with a Philips XL30 SEM equipped with EDAX on polished unetched sections. The composition measurements of each phase were performed on at least three testing points in order to ensure objectivity and later arithmetic means of these measured values were used as the representative composition of the phases. All the SEM images presented in this paper are back-scattered electron (BSE) images.

Table 1 Correspondence between mass fraction and mole fraction in $ICQ_{100-x}DQC_x$ pseudo-binary alloys

w / %		x / %		Composition of alloys (mole fraction, %)
IQC	DQC	IQC	DQC	
90	10	89.2	10.8	$Al_{62.9}Cu_{22.7}Fe_{11.1}Co_{1.6}Ni_{1.6}$
80	20	78.5	21.5	$Al_{63.7}Cu_{20.0}Fe_{9.8}Co_{3.2}Ni_{3.2}$
70	30	68.1	31.9	$Al_{64.6}Cu_{17.4}Fe_{8.5}Co_{4.8}Ni_{4.8}$
50	50	47.8	52.2	$Al_{66.2}Cu_{12.2}Fe_{6.0}Co_{7.8}Ni_{7.8}$
40	60	37.9	62.1	$Al_{67.0}Cu_{9.7}Fe_{4.7}Co_{9.3}Ni_{9.3}$
30	70	28.2	71.8	$Al_{67.7}Cu_{7.2}Fe_{3.5}Co_{10.8}Ni_{10.8}$
20	80	18.6	81.4	$Al_{68.5}Cu_{4.7}Fe_{2.3}Co_{12.2}Ni_{12.2}$
10	90	9.2	90.8	$Al_{69.3}Cu_{2.4}Fe_{1.2}Co_{1.2}Ni_{13.6}$

3 RESULTS

The X-ray diffraction (XRD) patterns carried out on ten annealed samples including the two initial quasicrystalline alloys and eight $IQC_{100-x}DQC_x$ alloys are illustrated in Fig. 1 respectively. And Fig. 2 presents the back-scattering electron (BSE) images of the eight pseudo-binary alloys, i.e. the $IQC_{100-x}DQC_x$ alloys, showing the morphology of the identified phases. The compositions of the identified phases are listed in Table 2. The valence electrons per atom values, e/a, of each phase are also listed in the table for reference. From IQC to DQC, three important approximants were involved in the whole transition process: AlFe-type β phase,

Table 2 Compositions and e/a values of phases identified in $IQC_{100-x}DQC_x$ alloys

w (IQC) / %	w (DQC) / %	τ3-Al_3Ni_2		λ-$Al_{13}Fe_4$	
		Composition (mole fraction%)	e/a	Composition (mole fraction, %)	e/a
90	10	$Al_{54.2}Cu_{33.9}Fe_{7.8}Co_{7.8}Ni_{2.6}$	2.20	$Al_{73.7}Cu_{4.7}Fe_{17.7}Co_{2.7}Ni_{1.2}$	2.09
80	20	$Al_{56.3}Cu_{30.8}Fe_{5.1}Co_{2.4}Ni_{5.3}$	2.22	$Al_{73.5}Cu_{5.1}Fe_{15.2}Co_{4.4}Ni_{1.8}$	2.09
70	30	$Al_{64.5}Cu_{20.6}Fe_{6.7}Co_{4.3}Ni_{3.9}$	2.22	$Al_{73.6}Cu_{73.6}Fe_{73.6}Co_{73.6}Ni_{2.3}$	2.10
50	50	$Al_{2.3}Cu_{2.3}Fe_{2.3}Co_{6.1}Ni_{11.7}$	2.13	$Al_{74}Cu_{74}Fe_{7.3}Co_{10.7}Ni_{3.9}$	2.08
40	60	$Al_{61.1}Cu_{18.4}Fe_{2.0}Co_{5.4}Ni_{13.1}$	2.10	$Al_{73.3}Cu_5Fe_{9.3}Co_{9.3}Ni_{9.3}$	2.08
30	70	$Al_{67.2}Cu_{7.8}Fe_{2.5}Co_{9.5}Ni_{13.1}$	2.01	$Al_{70}Cu_{5.6}Fe_{3.3}Co_{3.3}Ni_{8.4}$	2.00
20	80	$Al_{64.7}Cu_{8.6}Fe_{1.7}Co_{6.9}Ni_{18.1}$	2.00	$Al_{71.7}Cu_4Fe_{3.5}Co_{12.5}Ni_{8.3}$	2.02
10	90	$Al_{63.9}Cu_{6.6}Fe_{1.0}Co_{5.9}Ni_{22.7}$	1.96		

w (IQC) / %	w (DQC) / %	IQC		DQC	
		Composition (mole fraction%)	e/a	Composition (mole fraction, %)	e/a
90	10	$Al_{62.9}Cu_{24.3}Fe_{10.2}Co_{1.4}Ni_{1.2}$	2.25		
80	20	$Al_{63.9}Cu_{22.6}Fe_{9.3}Co_{2.4}Ni_{1.8}$	2.24	$Al_{67}Cu_{15.8}Fe_{9.1}Co_{4.4}Ni_{3.7}$	2.17
70	30			$Al_{68}Cu_{12.8}Fe_{7.3}Co_{6.1}Ni_{5.9}$	2.14
20	80			$Al_{71.9}Cu_{3.4}Fe_{2.5}Co_{12.5}Ni_{9.7}$	2.03
10	90			$Al_{71.1}Cu_{2.8}Fe_{0.9}Co_{0.9}Ni_{12.4}$	2.00

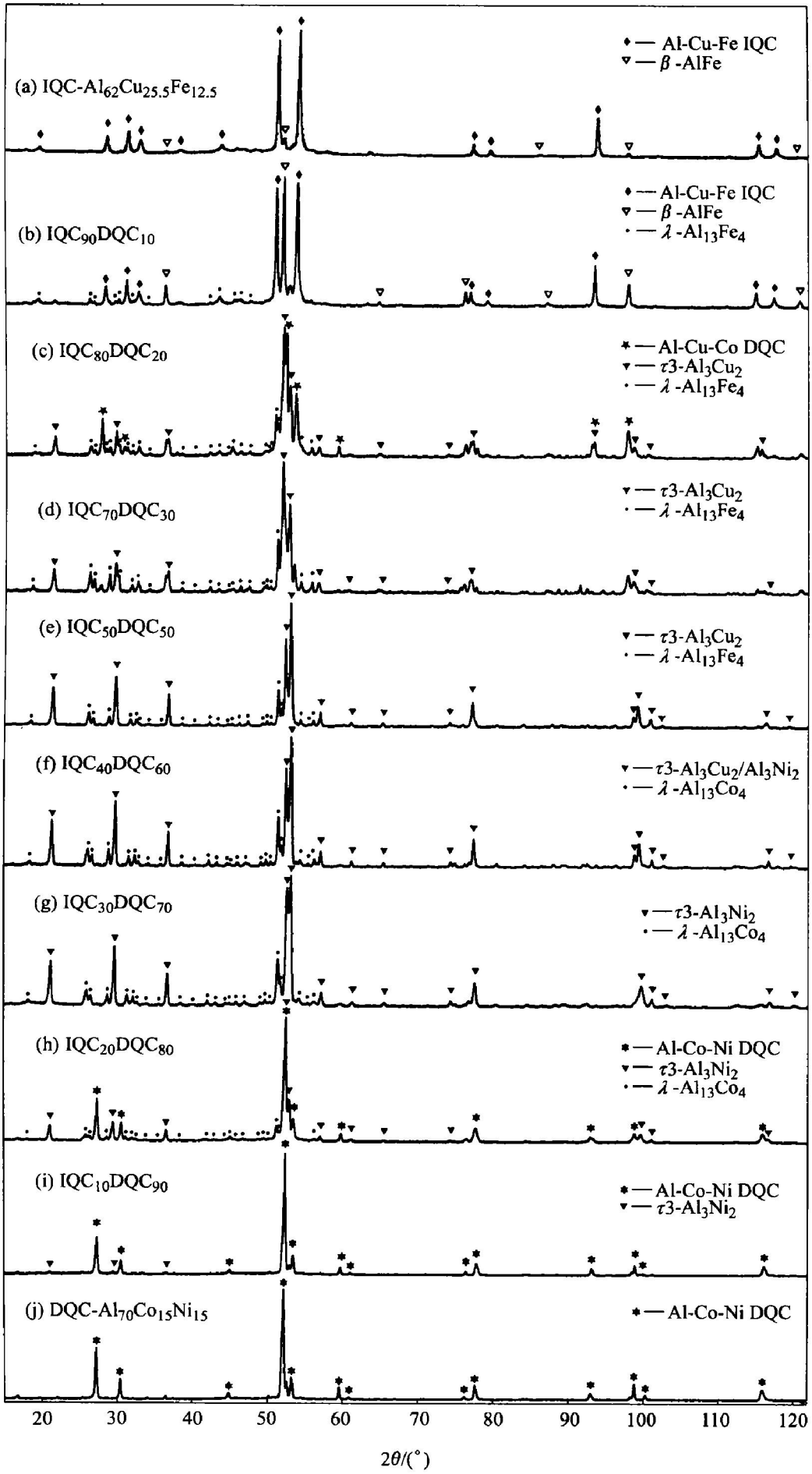

Fig. 1 XRD patterns of annealed $IQC_{100-x}DQC_x$ alloys, (a) —x = 0; (b) —x = 10; (c) —x = 20; (d) —x = 30; (e) —x = 50; (f) —x = 60; (g) —x = 70; (h) —x = 80; (i) —x = 90; (j) —x = 100

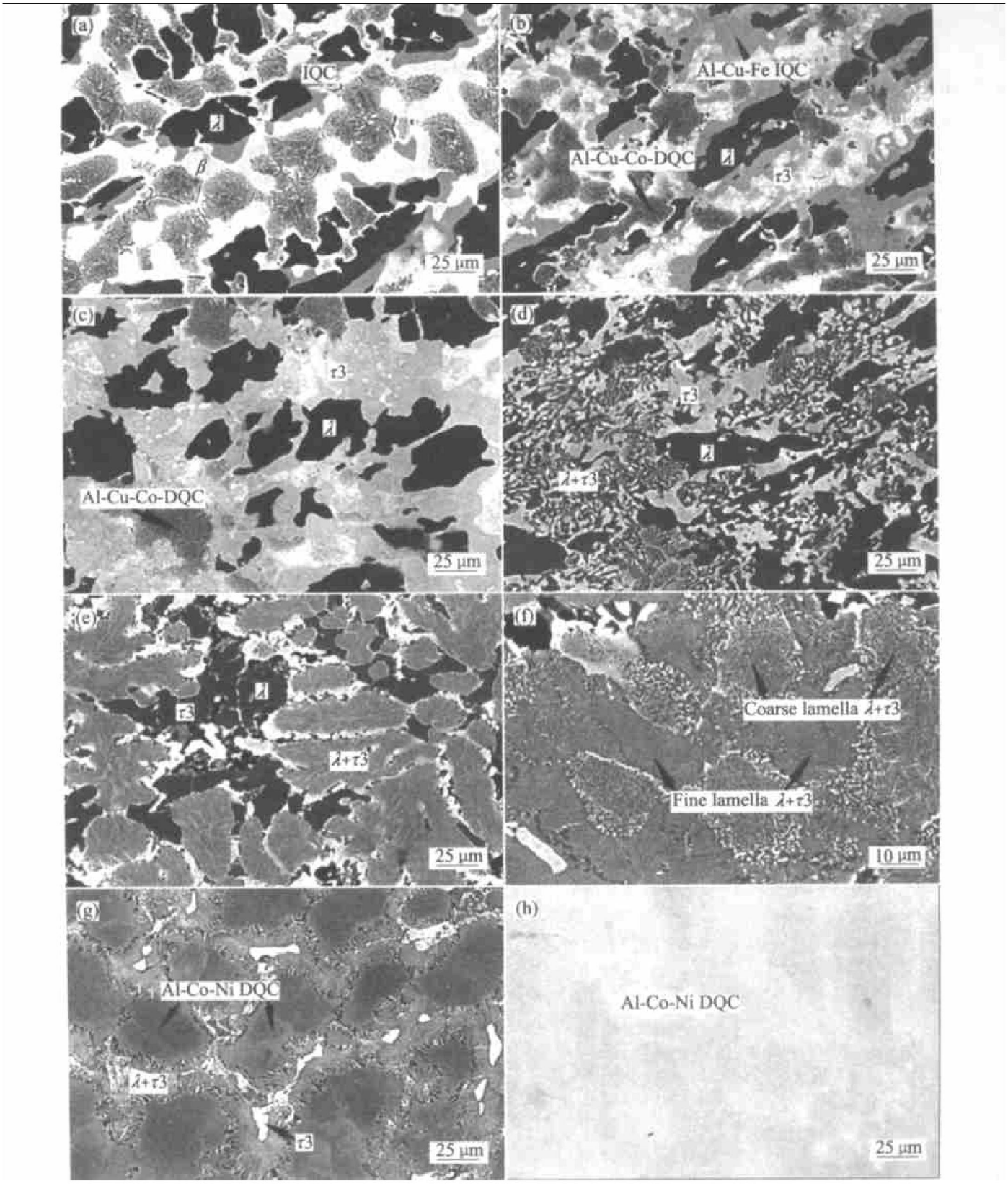

Fig. 2 SEM BSE images of $IQC_{100-x}DQC_x$ alloys after annealing at 1 023 K for 1 h
(a) —x = 10; (b) —x = 20; (c) —x = 30; (d) —x = 50; (e) —x = 60; (f) —x = 70; (g) —x = 80; (h) —x = 90

$Al_{13}Fe_4$-type λ phase and Al_3Ni_2-type τ3 phase. These phases will be referred to as β, λ and τ3 in the rest of the paper. Details about the structures, compositions and morphologies of the identified phases are presented in the following sections for all the $IQC_{100-x}DQC_x$ (x = 0, 10, 20, 30, 50, 60, 70, 80, 90 and 100) alloy.

3.1 Annealed initial IQC-$Al_{62}Cu_{25.5}Fe_{12.5}$ and DQC-$Al_{70}Co_{15}Ni_{15}$ alloys

As shown in Fig. 1(a), the initial Al-Cu-Fe IQC sample with the nominal composition of $Al_{62}Cu_{25.5}Fe_{12.5}$ still contains a small amount of the β phase after annealing. The measured composition of the IQC phase is $Al_{61.5}Cu_{27.7}Fe_{10.8}$. On the contrary, in Fig.

1(j), the XRD of the other initial alloy $Al_{70}Co_{15}Ni_{15}$ exhibits a pure DQC structure without any additional crystalline phase. Its measured composition is $Al_{70.8}Co_{14.8}Ni_{14.4}$.

3.2 $IQC_{90}DQC_{10}$ alloy

From the XRD pattern in Fig. 1 (b), its constituent phases are identified to be β, IQC and λ, among which the β phase is the predominant phase. In the corresponding BSE images (Fig. 2(a)), areas with dark, gray and white contrast correspond respectively to the λ phase, the IQC phase and the β phase. In addition to these identified phases, there exists a unidentified area with fine lamellar structure. Due to its fine structure, only average composition can be obtained: $Al_{61.5}Cu_{23.3}Fe_{10.1}Co_{2.4}Ni_{2.7}$, which is very close to the IQC composition.

3.3 $IQC_{80}DQC_{20}$ alloy

Different from the phase content in the previous alloy, in the alloy with 20% DQC content, the β phase is replaced by a τ3 phase (Fig. 1(c)). In addition to the λ and τ3 phases, a phase which is absent in the as-cast alloy has been identified from the XRD pattern (Fig. 1(c)) with peak positions similar to DQC-$Al_{65}Cu_{20}Co_{15}$. The BSE image of this alloy (Fig. 2(b)) is similar to that of IQC_{90}-DQC_{10} alloy (Fig. 2(a)): the phase with black contrast corresponds to the λ phase, and the phase with white contrast corresponds to the τ3 phase. The phase locates next to the λ phase and connects with the τ3 phase with gray contrast is identified to be the IQC phase. This IQC phase is hardly detectable in the XRD pattern due to its small volume fraction and overlapped diffraction peaks with the newly formed DQC phase. In the region containing fine lamella structure, the measured average composition is $Al_{67}Cu_{15.8}Fe_{9.1}Co_{4.4}Ni_{3.7}$, different from the similar structure in the $IQC_{90}DQC_{10}$ alloy. In its composition, it is worth to note that the mole ratio of (Cu+Ni) to (Fe+Co) is close to that of Cu to Co in the DQC-$Al_{65}Cu_{20}Co_{15}$ phase.

3.4 $IQC_{70}DQC_{30}$ alloy

From the XRD pattern (Fig. 1(d)), λ and τ3 are identified as the major component phases. Weak diffraction peaks corresponding to the DQC-$Al_{65}Cu_{20}Co_{15}$ phase could also be found. From its BSE image (Fig. 2(c)), the area with white contrast is identified to be τ3 and the one with dark contrast to be λ. The volume fractions of these two phases are approximately equal. The measured average composition of areas containing fine lamella structure is $Al_{68}Cu_{12.8}Fe_{7.3}Co_{6.1}Ni_{5.9}$, close to the composition of the similar structure in the IQC_{80}-DQC_{20} alloy. The volume fraction of the area with this morphology is relatively small. The weak diffraction peaks with DQC structure in the diffraction pattern have thus been identified as that originated from this lamellar structure.

3.5 $IQC_{50}DQC_{50}$ alloy

The XRD pattern (Fig. 1(e)) exhibits only two phases: λ and τ3. The intensity of the peaks indicates a large volume fraction of the τ3 phase in the alloy. In the BSE image (Fig. 2(d)), the area with black contrast is identified to be the λ phase. The area with black and white lamella structure contains two phases. The white lamellae are identified as τ3 phase and the black lamella as λ phase since their compositions coincide with those of the previous λ phase with black contrast.

3.6 $IQC_{40}DQC_{60}$ alloy

The XRD pattern of this alloy (Fig. 1(f)) is almost the same as that of the $IQC_{50}DQC_{50}$ alloy and can also be indexed with λ and τ3. The high diffraction peaks of τ3 indicate that this phase is the predominant phase in the alloy. In its BSE image (Fig. 2(e)), the area with dark gray contrast is identified as λ phase. Fine lamellar structure is found to be a common structure in the alloy. Phases with white contrast surrounding the fine structure are identified as τ3 phase. The fine structure has an average composition of $Al_{50}Cu_{12.3}Fe_{12.3}Co_{12.3}Ni_{8.5}$ which lies between λ and τ3 and is supposed to be composed of a mixture of these two phases by analogy with the $IQC_{50}DQC_{50}$ alloy. Therefore fine lamellae with gray contrast are thus identified as λ phase and lamellae with white contrast as τ3 phase.

3.7 $IQC_{30}DQC_{70}$ alloy

The same phases as identified in the IQC_{50}-DQC_{50} and $IQC_{40}DQC_{60}$ alloys are observed: λ and τ3 (Fig. 1(g)). From its corresponding BSE image (Fig. 2(f)), the fine lamella structure is predominant in this alloy and grains with size of 20 μm can be observed. Detailed study of their coarse lamella revealed that the white lamella can be identified as τ3 and the black lamella as λ. The average composition of the fine lamella phases is $Al_{69.2}Cu_6Fe_{3.6}Co_{10.7}Ni_{10.6}$, close to the DQC composition.

3.8 $IQC_{20}DQC_{80}$ alloy

In the XRD pattern of $IQC_{20}DQC_{80}$ alloy (Fig. 1(h)), in addition to the τ3 and λ phases, a DQC phase from the Al-Co-Ni system can also be observed. In its BSE image (Fig. 2(g)), a similar lamella grain structure as that in the $IQC_{30}DQC_{70}$ alloy can also be seen in this alloy with the difference that the black and white mixed structure is located at the grain boundaries only. The white phase is identified as τ3

and the black phase as λ. The center of the grains with gray contrast is identified as a DQC phase. Noticing that the compositions of λ and DQC are almost the same in this alloy, it is deduced that the λ phase is derived from the previous DQC phase before annealing.

3.9 $IQC_{10}DQC_{90}$ alloy

This alloy is composed of a nearly pure DQC phase with measured composition $Al_{71.1}Cu_{2.8}Fe_{0.9}Co_{12.8}Ni_{12.4}$ (Fig. 2(h) and (Fig. 1(i)).

4 DISCUSSION

4.1 Approximants in $IQC_{100-x}DQC_x$ alloys

In almost every intermediate alloy, approximants λ and τ3 are closely related with the transition process. Theoretically, these approximants are all closely related with the formation of their corresponding QCs.

The monoclinic λ phase is a complex approximant phase. It possesses successive pseudo-icosahedral layered structure similar to that of α-AlMnSi IQC[7]. It is also considered a prototype to model decagonal phases because of its pseudo-quasiperiodic distribution of the atoms in the layer perpendicular to the *b*-axis. It is therefore considered to be an approximant phase to both types of QCs.

As to the crystalline phases with B2-based structure such as β-AlFe and τ3-Al_3Ni_2, they are related to QCs via similar *e*/*a* values and are thus also considered to be approximants[8]. Although they have only simple structures, the two phases also possess certain structural correlations with QCs. The structure of τ3-Al_3Ni_2 can be described by a six-layered stacking of (102) planes that correspond to the quasiperiodic planes of the decagonal phase[9]. As to the β phase, its local atomic structure is found to resemble that of QCs[8]: atoms on β-{110} planes, which is parallel to the 5- or 10-fold planes of QCs, can be linked to a Penrose tiling type of network. The pseudo-5-fold or 10-fold symmetry is thus present even in the B2-based structures. These approximants are all Humer-Rothery phases.

4.2 Formation of Al-Cu-Co DQC phase in $IQC_{80}DQC_{20}$ alloy

The most interesting result in this work is the appearance of a Al-Cu-Co DQC phase with 20% DQC (mass fraction) deviation from the Al-Cu-Fe IQC alloy. The formation of this QC phase in annealed $IQC_{80}DQC_{20}$ alloy proves that even intensive alloying process was applied, and the icosahedron or near icosahedron atomic configurations were still retained in the alloy.

As it is well known, the Al-Cu-Co DQC phase is a stable decagonal phase having similar atomic structure to the Al-Co-Ni DQC. According to Steurer et al[14], these two decagonal phases share similar decaprismatic clusters and their columnar structure along the ten-fold screw axis are all characterized by the same 4 Å translation period. The similar XRD patterns (Fig. 1(c) and (h)) confirm the similarity in their structures.

In Table 2, *e*/*a* values of constituent phases are calculated according to their measured compositions in each alloy. It is discovered that all the phases formed in pseudo-binary alloys have very close *e*/*a* values. It is also worth to mention that the intense peak positions of the main constituent phase in the XRD patterns of these alloys are nearly unchanged. These peak positions actually define the dimensions of the Brillouin zones in contact with the Fermi spheres.

All the above findings indicate that the formation of icosahedral cluster in these pseudo-binary alloys still follows the Humer-Rothery rule. The alloying process has in fact destroyed the quasiperiodic arrangement of the icosahedra and transformed it into periodic or partially periodic arrangements of these icosahedra. This result indicates that the introduction of different size or type of clusters can be considered an effective way of introducing disorders into the original perfect lattices and leading to the formation of more disordered structures.

4.3 Al-(Cu, Ni)-(Fe, Co) pseudo-ternary phase diagram

A pseudo-ternary phase diagram Al-(Cu, Ni)-(Fe, Co) (Fig. 3) has been constructed to explain the phase formation sequences in the IQC_{100-x}-DQC_x alloy series. Composition points representing two starting QCs, namely IQC-$Al_{61.5}Cu_{27.7}Fe_{27.7}$ and DQC-$Al_{70.8}Co_{14.8}Ni_{14.4}$ are marked in the figure. Their corresponding *e*/*a*-constant lines are also drawn in the figure. Composition points representing the eight intermediate $IQC_{100-x}DQC_x$ alloys are also indicated. It is obvious to find that the eight intermediate composition points forms a straight line linking the composition points of the two initial QCs. One composition point representing the newly formed Al-Cu-Co DQC is also marked in the diagram.

The calculation of *e*/*a* values from measurement compositions of constituent phases proves that there exists a tendency of evolution of their corresponding *e*/*a*-constant lines from the IQC line to the DQC line. And the formation of constituent phases in each alloy would also follow the evolution of their corresponding *e*/*a*-constant lines. At the IQC end, the phase formation would follow the rule in the Al-Cu-Fe alloy system: their main constituent is IQC with β and λ. When the DQC content

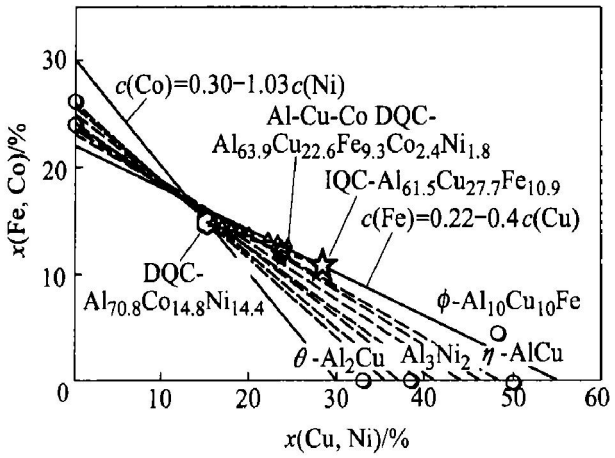

Fig. 3 Al-(Cu, Ni)-(Fe, Co) pseudo-ternary phase diagram

increases, the composition of these constituent phases will also change towards phases in the DQC alloy system: the λ-$Al_{13}Fe_4$ phase is gradually replaced by $Al_{13}Co_4$ and τ3-$Al_{10}Cu_{10}Fe$ phase replaced by τ3-Al_3Ni_2. These findings have additionally proved the effectiveness of the Humer-Rothery rule in QC related alloy systems.

5 CONCLUSIONS

After investigation of the phases formed after annealing in the $IQC_{100-x}DQC_x$ alloys, the following conclusions can be drawn:

1) The addition of the Al-Co-Ni DQC into the Al-Cu-Fe IQC have effectively broken the original quasiperiodic lattice structures and produces mainly approximants: λ-$Al_{13}Fe_4$, τ3-Al_3Ni_2 and β-AlFe.

2) The formation of the approximant phases in the intermediate alloys is characterized by constant-e/a feature and follows the corresponding e/a-constant lines between the two lines representing the two initial QCs in the pseudo-ternary Al-(Cu, Ni)-(Fe, Co) phase diagram.

3) Icosahedron or near icosahedron atomic configurations are still retained in the resulted approximant phase after the alloying process. The formation of icosahedral cluster in these pseudo-binary alloys is still governed by the Humer-Rothery rule.

REFERENCES

[1] Sanchez-Pascual A, Garcia de Blas F J, Algaba J M, et al. Applications of quasicrystalline materials as thermal barriers [A]. Dubois J M, Thiel P A, Tsai A P, et al. MRS Symposium Proceedings [C]. Warrendale, PA: 1999. 447-452.

[2] Eisenhammer T, Lazarov M. Radiation converter made from quasicrystalline material [P]. German Patent 4425140. 1995.

[3] Dubois J M, Machizaud F. Devices for the absorption of the infrared radiation made by quasicrystalline alloy lens element [P]. French Patent 2744839. 1995.

[4] Cyrot-Lackmann F, Grenet T, Berger C, et al. Thin layered lenses made of quasicrystalline alloys, their application and uses [P]. French Patent 2732697. 1995.

[5] Kelton K F, Viano A M, Stroud R M, et al. Hydrogen storage in Ti-based quasicrystals [A]. Goldman A I, Sordelet D J, Thiel P A, et al. New Horizons in Quasicrystals: Research and Applications [C]. Singapore: World Scientific, 1997. 272-279.

[6] Zander D, Koster U, Eliaz N, et al. Influence of hydrogen on formation and stability of Zr-based quasicrystals [J]. Materials Science and Engineering A, 2000, 294-296: 112-115.

[7] Elser V, Henley C L. Crystal and quasicrystal structures in Al-Mn-Si alloys [J]. Phys Rev Lett, 1985, 55(26): 2883-2886.

[8] Dong C, Zhang L M, Zhou Q G, et al. Structure and tribological property of B2-based approximants [J]. Bull Mater Sci, 1999, 22(3): 465-472.

[9] Dong C. The Al_3Ni_2 structure as approximant of quasicrystals [J]. J Phys I France, 1995, 5: 1625-1634.

[10] Dong C. The concept of the approximants of quasicrystals [J]. Scrip Met Mater, 1995, 33(2): 239-243.

[11] Schaefer R J, Bendersky L. Replacement of icosahedral Al-Mn by decagonal phase [J]. Scrip Met, 1986, 20(5): 745-750.

[12] Hiraga K, Sun W, Lincoln F J, et al. Formation of decagonal quasicrystal in the Al-Pd-Mn system and its structure [J]. Japan J Appl Phys, Part 1, 1991, 30(9A): 2028-2034. (in Japanese)

[13] Kang S S, Dubois J M. Influence of the annealing atmosphere on the formation of Al-Cu-Fe quasicrystals [J]. Mater Res, 1995, 10(5): 1071-1074.

[14] Steurer W. Comparative structure analysis of several decagonal phases [J]. J Non-Cryst Solids, 1993, 153-154: 92-97.

(Edited by YANG Bing)